Electronic Supplementary Information 6

Analytical approximation for the Poisson-Boltzmann solution in the solid nanochannel model

Introduction

Although no general solution to the Poisson-Boltzmann equation is known, a number of analytical approximations are available in the literature for particular conditions. This namely involves local conditions where the electric potential largely exceeds the thermal potential V_{th}, or is largely below this value.

Providing analytical approximations has the strong merit to outline general tendencies difficult to understand from purely numerical simulations. It is namely of interest to have simple expressions for the electric potential at the channel midline and in the immediate vicinity of the alginate strands, to globally define the overall state in terms of double layer overlap and order of magnitude of maximum potentials encountered. In the context of the main text, the analytical approximations are applicable to the "solid nanochannel" model. Indeed, for historical reasons, much of the literature work on polyelectrolytes is based on a geometry where a small, highly charged fixed space charge region is bounded by a solution devoid of any fixed space charge.

In our experimental conditions, we generally find regions where $|\Phi|>>V_{th}$, and regions where on the contrary $|\Phi|<<V_{th}$. In particular, near the alginate strands, we expect highly negative values for the electric potential, on the order of several $-V_{th}$. Near the channel midline, we expect lower electric potential values, which may or may not fulfill $|\Phi|<<V_{th}$, depending on the pore size and free salt concentration. In fact, whether or not $|\Phi|$ drops below V_{th} allows to define to regimes: in the strong double layer overlap regime, $|\Phi|$ remains above V_{th} everywhere in the channel, whereas in the weak overlap regime, part of the channel along the symmetry axis is characterized by an electric potential below the thermal voltage V_{th}.

Given that no global solution to the Poisson-Boltzmann equation is known, it is therefore necessary to delimit and analyze the different regions independently. However, once this analysis is done, we can still use a common expression for the partition coefficient K based on the relevant potentials at the channel walls and midline.

Overview over the main approach and equations

This section gives a rough outline over the overall analytical approach carried out in this Electronic Supplementary Information. It should allow to rapidly locate the most relevant equations.

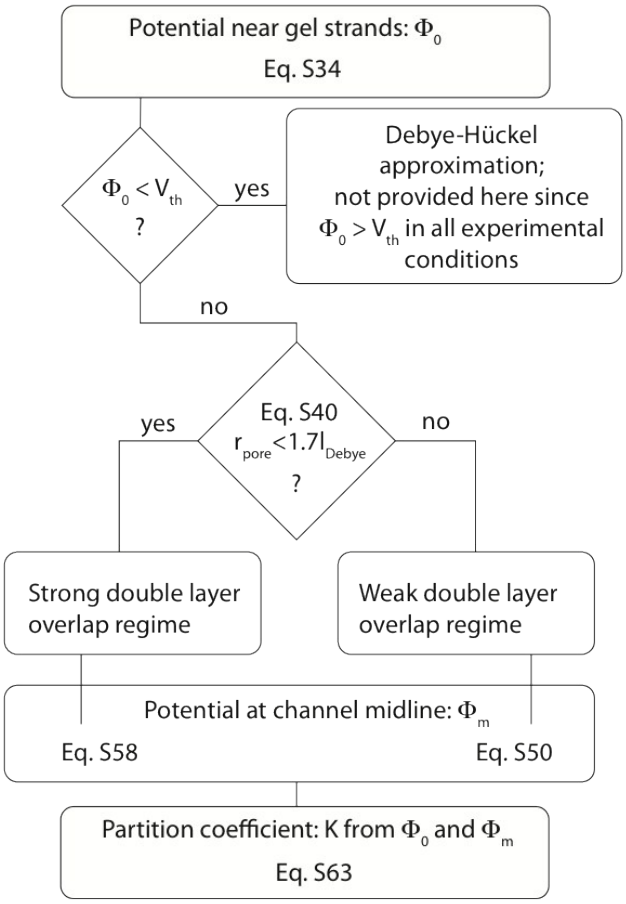

Fig. S31: General approach to analytical characterization of potential distribution and partition coefficient for the "solid nanochannel" model. The equations indicated concern directly the experimental conditions for the alginate hydrogels, the reader will also find more generic versions throughout the development in this electronic supplementary information section if necessary.

Fig. S31 shows the approach taken to the determination of the partition coefficient by analytical equations within the framework of the "solid nanochannel" model. The development follows the general outline given by Overbeek[1] in that we evaluate the electric potentials Φ_0 at the channel walls and Φ_m at the channel midline using appropriate simplifications, to then evaluate the partition coefficient K from a common final equation. We explicitly do not include the otherwise well-known case where $|\Phi|$ does not exceed the thermal voltage V_{th} (the Debye-Hückel theory[2]) as we do not encounter this condition experimentally.

The algorithm indicated in Fig. S31 is implemented in the poisson.boltzmann.1D package available as Electronic Supplementary Information from Soft Matter.

In terms of basic assumptions and notations, we follow Overbeek's development here, which means that generally Φ is negative (this is also the case for our alginate hydrogels), and the fixed space charge region is located to the right (it is to the left in the main text). This does not change the main conclusions nor absolute values obtained.

Surface potential Φ_0 near the alginate strands

Starting point of our analysis is the electric potential Φ_0 found near the alginate gel strands (the channel walls in terms of the solid nanochannel model).

Due to the electrostatic shielding by the mobile ions, we generally expect the local potential near a given alginate strand to be little influenced by all the other strands. Also, due to the high local potential, there is almost complete local exclusion of co-ions, such that it is enough to take the counter-ions into account. Adapting the development given by Overbeek[1] to these simplifications, we start out with a simplified Poisson-Boltzmann equation:

$$\frac{\mathrm{d}^2\Phi}{\mathrm{d}x^2} = -\frac{N_A q_e c_0}{\varepsilon_r \varepsilon_0} \cdot e^{-\Phi(x)/V_{th}} \qquad \text{(S32)}$$

where it is assumed that $\Phi << -V_{th}$ (and therefore $|\Phi| >> V_{th}$) in the relevant areas, such that the co-ion term of $\exp(\Phi/V_{th})$ can safely be neglected. Eq. S32 is the analog of eq. 33 in Overbeek's paper[1], using modern notation and neglecting the co-ion term.

In analogy to Overbeek's approach[1], integration of eq. S32 yields:

$$\frac{\mathrm{d}\Phi}{\mathrm{d}x} = -\sqrt{\frac{2k_B T \cdot N_A c_0}{\varepsilon_r \varepsilon_0}} e^{-\Phi(x)/2V_{th}} \qquad \text{(S33)}$$

Since $-\mathrm{d}\Phi/\mathrm{d}x$ represents the electric field, eq. S33 can be used to relate surface charge and surface potential[1] via Gauss's flux theorem:

$$\Phi_0 = -2V_{th} \ln\left[-\frac{\sigma}{\sqrt{2c_0\varepsilon_0\varepsilon_r \cdot k_B T N_A}}\right] \approx -2V_{th} \ln\left[\frac{3.7}{\sqrt{c_0[\mathrm{M}]}}\right] \qquad \text{(S34)}$$

In eq. S34, we have also provided a numerical evaluation for our specific case. Indeed, from the relation between pore size and alginate concentration given in Fig. 3 in the main text (i.e. $d_{pore}=2r_{pore}=877\mathrm{nm}/c[\mathrm{mg/mL}]$), one can estimate an effective alginate strand diameter of about 0.6nm. This is done by noting that the volume fraction will be given by c[mg/mL]/(1500mg/mL), when a specific density of 1.5kg/l is assumed for the alginate, and the wall diameter will be the

pore diameter times the volume fraction (i.e. 877nm/(mg/mL)/c*c/(1500mg/mL)=877nm/1500=0.6nm). Together with a molecular weight of 200g/mol per charge, one obtains an effective surface charge density of about σ=0.22C/m^2 for each of the two pores bounding a wall (i.e. the molar concentration of charged hexose residues within the walls is 1500g/L/200g/mol=7.5M; this corresponds to a fixed charged density of 7500mol/m^3*6.022*10^{23} charges/mol*1.6*10^{-19}C/charge=7.2*10^{8}C/m^3; with a wall thickness of 0.6nm, this gives an overall surface charge density of 7.2*10^{8}C/m3*0.6*10^{-9}m=0.43C/m^2; this is distributed among the 2 lining pores, such that the relevant charge density is 0.22C/m^2). Given that the maximum free salt concentration c_0 used throughout this study is 1M, eq. S34 confirms that $|\Phi_0|$ significantly exceeds V_{th}=25mV in all conditions. Indeed, as estimated by eq. S34, Φ_0 ranges from -67mV at 1M to -240mV at 1mM free salt concentration. Eq. S34 further expresses a logarithmic dependence of the surface potential on the charge density σ, in accordance with the developments by Manning[3].

Determination of the double layer overlap regime

The next step is to determine whether weak or strong double layer overlap occurs. The two regimes are illustrated in Fig. S35. We refer to weak double layer overlap if the electric potential drops below an absolute value of V_{th} towards the channel midline (Fig. S35-A) and to strong double layer overlap if the absolute value of the potential never drops below the thermal voltage V_{th} (Fig. S35-B). The goal of this section is therefore to determine under what conditions $|\Phi|$ drops below V_{th}≈25mV.

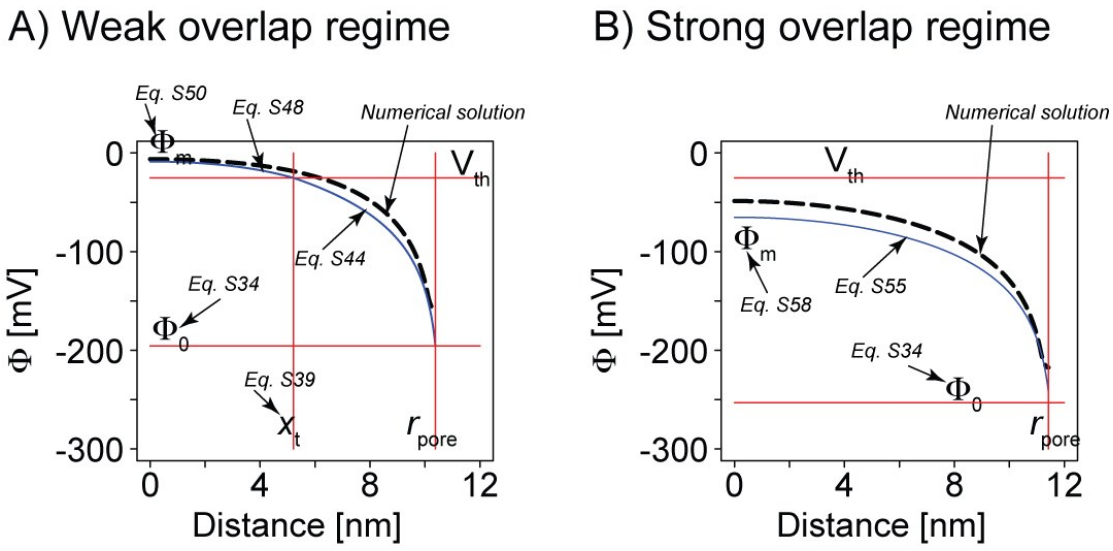

Figure S35: Weak and strong double layer overlap regime. In the weak overlap regime (A), $|\Phi|$ drops below V_{th} towards the channel midline (near x=0), whereas in the strong overlap regime (B), it does not. The figure also indicates the relevant variables and the equations used to calculate the corresponding values or the corresponding trace.

As a first step, we integrate equation S33 by separation of variables. We should however only apply S33 to the region close to the channel walls where indeed $\Phi<V_{th}$ remains valid. In the strong double layer overlap regime, this will be everywhere, but in the weak double layer overlap regime, there will be a critical position x_t such that at $x=x_t$, $\Phi=-V_{th}$. For the moment, we shall suppose that such a position x_t exists. Integration then yields:

$$\int_{\Phi=-V_{th}}^{\Phi=\Phi_0} \exp\left(\Phi(x)/2V_{\text{th}}\right)\mathrm{d}\Phi = -\int_{x=x_t}^{x=r_{pore}} \sqrt{\frac{k_B T\cdot N_A c_0}{\varepsilon_r \varepsilon_0}}\mathrm{d}x \tag{S36}$$

and therefore:

$$2V_{th}\left[\exp(-1/2)-\exp\left(\Phi_0/2V_{\text{th}}\right)\right]=\sqrt{\frac{k_B T\cdot N_A c_0}{\varepsilon_r \varepsilon_0}}\cdot\left(r_{pore}-x_t\right) \tag{S37}$$

We can isolate an expression for the width of the region where $\Phi>V_{th}$ remains valid:

$$r_{pore}-x_t = 2\sqrt{2}\cdot l_{Debye}\cdot\left[\exp(-1/2)-\exp\left(\Phi_0/2V_{\text{th}}\right)\right] \tag{S38}$$

Under our experimental conditions, we always have $\Phi_0<-3V_{th}$, allowing to neglect the second exponential in eq. S38. Ultimately, we can therefore estimate the width of the high-potential region around the alginate fibers to:

$$\Delta x = r_{pore}-x_t \approx 2\sqrt{2}\exp\left(-\frac{1}{2}\right)\cdot l_{\text{Debye}} \approx 1.7 l_{\text{Debye}} \tag{S39}$$

Eq. S39 explicitly describes a particularity of the solutions to the Poisson-Boltzmann equation involving islands of highly concentrated fixed charge density. Indeed, it appears from the numerical solutions that the width of the peak in the electric potential that is associated with such charged islands depends little on the absolute charge density within the islands. Merely, higher island charge seems to be associated with high electric potential peaks, but not larger ones. Eq. S39, taken in the limit of high electric potential and thus high charge density, indicates that the potential will drop to values on the order of the thermal voltage V_{th} within two Debye lengths from the edge of the island, regardless of the absolute charge density within the island.

Eq. S39 also allows to quantitatively distinguish low and high double layer overlap regimes. Indeed, if $r_{pore}<1.7 l_{Debye}$, x_t becomes negative and thus physically irrelevant, indicating high double layer overlap and $|\Phi|>V_{th}$ everywhere. A low energy region with $|\Phi|<V_{th}$ extending from the channel midline (x=0) to $x=r_{pore}-1.7 l_{Debye}$ will exist only if $r_{pore}<1.7 l_{Debye}$, defining the low double layer overlap regime. Succinctly, we can therefore note:

$$\begin{cases} r_{\text{pore}} < 1.7 l_{\text{Debye}} \Rightarrow \text{strong double layer overlap} \\ r_{\text{pore}} >= 1.7 l_{\text{Debye}} \Rightarrow \text{weak double layer overlap} \end{cases} \tag{S40}$$

Weak double layer overlap regime

For the weak overlap regime, we should use boundary conditions reflecting the transition from a high potential to a low potential region at $x=x_t$ as defined by equation S39. The simultaneous existence of a low potential region from $x=0$ to $x=x_t$ along with a high potential region from $x=x_t$ to $x=r_{pore}$, implies indeed a separate analysis for the two sub-regions.

For the high potential region between $x=x_t$ and $x=r_{pore}$, we need to solve eq. S33.

We proceed by separation of variables as before:

$$\int_{-V_{th}}^{\Phi} \exp\left(\Phi/2V_{th}\right)\mathrm{d}\Phi = -\int_{x_t}^{r_{pore}} \sqrt{\frac{k_B T\cdot N_A c_0}{\varepsilon_r \varepsilon_0}}\mathrm{d}x \tag{S41}$$

which yields:

$$x - x_t = 2\sqrt{2}l_{Debye}\cdot\left[\exp\left(-\frac{1}{2}\right) - \exp\left(\frac{\Phi}{2V_{th}}\right)\right] \tag{S42}$$

from which we isolate:

$$\Phi = 2V_{th}\ln\left(-\frac{x-x_t}{2\sqrt{2}l_{Debye}} + \exp\left(-\frac{1}{2}\right)\right) \tag{S43}$$

By use of eq. S38, we further obtain:

$$\Phi = 2V_{th}\ln\left(\exp\left(-\frac{1}{2}\right)\cdot\frac{r_{pore}-x}{r_{pore}-x_t} + \exp\left(\frac{\Phi_0}{2V_{th}}\right)\cdot\frac{x-x_t}{r_{pore}-x_t}\right) \tag{S44}$$

showing the logarithmic transition for Φ from $-V_{th}$ to Φ_0 occurring on the interval from $x=x_t$ to $x=r_{pore}$.

For the low potential region towards the channel midline, we can use the Debye-Hückel linearization of the Poisson-Boltzmann equation[2]:

$$\frac{\mathrm{d}^2\Phi}{\mathrm{d}x^2} = \frac{\Phi}{l_{\mathrm{Debye}}^2} \tag{S45}$$

valid in absence of fixed space charge, and wherever $|\Phi|<V_{th}$.

In this case, the solutions are well-known exponentials with decay constants of l_{Debye}. Imposing the boundary conditions

$$\left(\frac{\mathrm{d}\Phi}{\mathrm{d}x}\right)_{x=0} = 0 \tag{S46}$$

and

$$\Phi(x = x_t) = -V_{th} \tag{S47}$$

the solution reads:

$$\Phi = -V_{th} \cdot \cosh\left(\frac{x}{l_{\mathrm{Debye}}}\right) \Big/ \cosh\left(\frac{x_t}{l_{\mathrm{Debye}}}\right) \tag{S48}$$

and the electric potential at the channel midline $\Phi_m=\Phi(x=0)$ becomes:

$$\Phi_m = -V_{th} \Big/ \cosh\left(\frac{x_t}{l_{\mathrm{Debye}}}\right) \tag{S49}$$

for our particular case, this will be:

$$\Phi_m = -V_{th} / \cosh\left(\frac{r_{pore}}{l_{Debye}} - 2\sqrt{2} \cdot \exp(-1/2)\right) \approx -V_{th} / \cosh\left(\frac{r_{pore}}{l_{Debye}} - 1.7\right) \tag{S50}$$

Eq. S50 again underpins the idea that the exact charge density of the alginate strands is much less important for the events near the channel midline than the fundamental ratio of channel size to Debye screening length.

Strong double layer overlap regime

The strong double layer overlap regime occurs when $r_{\mathrm{pore}}<1.7*l_{\mathrm{Debye}}$. In this case, $|\Phi|$ does not drop to V_{th} anywhere in the channel, and we are looking for a single solution on the entire interval $x=0$ to $x=r_{\mathrm{pore}}$. We need to keep the exponential dependence in the Poisson-Boltzmann equation. However, in this case, the contribution of the co-ions to the space charge can be neglected, and we can adapt of Overbeek's[1] formula 41, such as to be able to find an analytical solution. We therefore have:

$$\frac{\mathrm{d}\Phi}{\mathrm{d}x} = -\sqrt{\frac{k_B T \cdot N_A c_0}{\varepsilon_0 \varepsilon_r}} \cdot \sqrt{\exp\left(-\Phi/V_{th}\right) - \exp\left(-\Phi_m/V_{th}\right)} \tag{S51}$$

Eq. S51 is designed to yield $\mathrm{d}\Phi/\mathrm{d}x=0$ for $x=0$, since then $\Phi=\Phi_{\mathrm{m}}$, in order to respect the channel symmetry.

Eq. S51 can be integrated by separation of variables, one obtains:

$$\int_{\Phi_m}^{\Phi} \frac{\mathrm{d}\Phi}{\sqrt{\exp\left(-\Phi/V_{\mathrm{th}}\right)-\exp\left(-\Phi_m/V_{\mathrm{th}}\right)}} = -\int_0^x \sqrt{\frac{k_B T\cdot N_A c_0}{\varepsilon_r \varepsilon_0}}\mathrm{d}x \tag{S52}$$

which yields:

$$-2V_{th}\cdot \exp\left(\frac{\Phi_m}{2V_{th}}\right)\cdot \arctan\left(\sqrt{\exp\left(-\left(\Phi-\Phi_m\right)/V_{\mathrm{th}}\right)-1}\right) = -x\sqrt{\frac{k_B T\cdot N_A c_0}{\varepsilon_r \varepsilon_0}} \tag{S53}$$

From this, we can isolate an expression for Φ:

$$\Phi = \Phi_m + 2V_{th}\ln\left\{\cos\left[\frac{x}{2\sqrt{2}l_{\mathrm{Debye}}}\exp\left(\frac{-\Phi_m}{2V_{th}}\right)\right]\right\} \tag{S54}$$

Eq. S54 in particular allows to determine Φ_m. We can do so by setting $x=r_{\mathrm{pore}}$, and noting that in this case, we also must have $\Phi=\Phi_0$:

$$\Phi_0 = \Phi_m + 2V_{th}\ln\left\{\cos\left[\frac{r_{pore}}{2\sqrt{2}l_{\mathrm{Debye}}}\exp\left(\frac{-\Phi_m}{2V_{th}}\right)\right]\right\} \tag{S55}$$

In our case, Φ_m is still substantially smaller than Φ_0 even for strong double layer overlap. In this case, we have:

$$\Phi_0 \approx 2V_{th}\ln\left\{\cos\left[\frac{r_{pore}}{2\sqrt{2}l_{\mathrm{Debye}}}\exp\left(\frac{-\Phi_m}{2V_{th}}\right)\right]\right\} \tag{S56}$$

from which we isolate:

$$\Phi_m = -2V_{th}\ln\left\{\frac{2\sqrt{2}l_{\mathrm{Debye}}}{r_{pore}}\arccos\left[\exp\left(\frac{\Phi_0}{2V_{th}}\right)\right]\right\} \tag{S57}$$

Due to the high charge density associated with the alginate strands, we typically have values of Φ_0 of minus several V_{th} under the conditions of strong double layer overlap (which are also the conditions of low ionic strength). In that case, we can further simplify:

$$\Phi_m \approx 2V_{th}\ln\left\{\frac{2\sqrt{2}l_{\mathrm{Debye}}}{r_{pore}}\arccos[0]\right\} = -2V_{th}\ln\left\{\pi\sqrt{2}\,\frac{l_{\mathrm{Debye}}}{r_{pore}}\right\} \tag{S58}$$

Eq. S58 indicates that even in case of the strong double layer overlap regime, the exact value of the charge density has little influence on the electric potential far from highly charged regions. The physical interpretation is analogous to the one

given for eq. S39 for the weak overlap regime: most of the counter ions are concentrated in the small regions with very large potentials near the gel strands, shielding off most of the space charge. As a result, what happens towards the channel midline is much more strongly dominated by the ratio of the Debye length to the pore radius than the exact charge density on the walls.

Partition coefficient

The final goal of this Electronic Supplementary Information section is to obtain an expression for the partition coefficient *K*.

Regardless of whether we are facing strong or weak double layer overlap, we dispose of the characteristic potentials Φ_0 (from eq. S34) and Φ_m (either from eq. S50 or eq. S58) at this stage. We are now looking for a relation between these values and the partition coefficient *K*.

The partition coefficient *K* for a given ionic species is calculated by:

$$K^{n\pm} = \frac{1}{r_{\text{pore}}} \int_0^{r_{\text{pore}}} \mathrm{e}^{\mp n\Phi(x)/V_{\text{th}}} \mathrm{d}x$$

(eq. 8 in the main text)

This equation can obviously be evaluated if the distribution of the electric potential $\Phi(x)$ is known. However, even in the absence of a known analytical solution for $\Phi(x)$, Overbeek[1] proposes to use the known distribution of $\mathrm{d}\Phi(x)/\mathrm{d}x$, generically valid for strongly and weakly overlapping double layers. Indeed, by substitution of variables, we have:

$$K^{n\pm} = \frac{1}{r_{\text{pore}}} \int_{\Phi_m}^{\Phi_0} \mathrm{e}^{\mp n\Phi/V_{\text{th}}} \cdot \left(\frac{\mathrm{d}\Phi}{\mathrm{d}x}\right)^{-1} \cdot \mathrm{d}\Phi \qquad \text{(S59)}$$

This allows to make use the expression for $\mathrm{d}\Phi(x)/\mathrm{d}x$ for overlapping double layers, given by Overbeek[1] (reproduced here using modern notation):

$$\frac{\mathrm{d}\Phi}{\mathrm{d}x} = -\sqrt{\frac{2c_0RT}{\varepsilon_r\varepsilon_0}} \sqrt{\cosh\left(\Phi(x)/V_{\text{th}}\right) - \cosh\left(\Phi_m/V_{\text{th}}\right)} \qquad \text{(S60)}$$

such that the partition coefficient can be estimated according to:

$$K^{n\pm} = -\sqrt{\frac{\varepsilon_0\varepsilon_r}{2c_0RT}} \frac{1}{r_{\text{pore}}} \int_{\Phi_m}^{\Phi_0} \frac{\mathrm{e}^{\mp n\Phi/V_{\text{th}}} \cdot \mathrm{d}\Phi}{\sqrt{\cosh(\Phi/V_{\text{th}}) - \cosh(\Phi_m/V_{\text{th}})}} \qquad \text{(S61)}$$

which further yields by substitution for $y=\Phi/V_{\text{th}}$:

$$K^{n\pm} = -\frac{l_{\text{Debye}}}{r_{\text{pore}}} \int_{\Phi_m/V_{\text{th}}}^{\Phi_0/V_{\text{th}}} \frac{\mathrm{e}^{\mp ny} \cdot \mathrm{d}y}{\sqrt{\cosh(y) - \cosh(\Phi_m/V_{\text{th}})}} \qquad \text{(S62)}$$

As we are unable to find a general analytical solution to eq. S62, the integration must be carried out numerically. If Φ_0 and Φ_m are suitably chosen, the partition coefficient of a neutral substance (n=0) should be given by K^0=1. Since however Φ_0 and Φ_m are generally chosen by approximate formulae (i.e. equations S34, S50 or S58), we generally find deviations from K^0=1 when using eq. S62 for n=0, such that we prefer to normalize:

$$K^{n\pm} = \frac{\int_{\Phi_m/V_{th}}^{\Phi_0/V_{th}} e^{\mp ny} \left(\cosh(y) - \cosh(\Phi_m/V_{th})\right)^{-\frac{1}{2}} \cdot dy}{\int_{\Phi_m/V_{th}}^{\Phi_0/V_{th}} \left(\cosh(y) - \cosh(\Phi_m/V_{th})\right)^{-\frac{1}{2}} \cdot dy} \qquad \text{(S63)}$$

Eq. S63 is reported as eq. 10 in the main text.

Thus, we can estimate the partition coefficient K for an ion of any valence n, without the explicit knowledge of the exact analytical formula for $\Phi(x)$, merely from the values of Φ_0 and Φ_m, by numerical integration of eq. S63. The physical interpretation of Eq. S63 is that it provides a suitably weighted mean of the local partition coefficients given by $\exp(-n\Phi/V_{th})$.

Comparison to numerical simulation

It is finally of interest to compare the numerical simulation and analytical approximation formulae. This basically allows to double-check the two distinct approaches against each other, and gives an estimate of the precision of the analytical approximations.

We have done so for the twelve experimental conditions (the three gel concentrations at synthesis, and the 4 bulk KCl concentrations used through the main text), for the electric potential near the alginate strands (Φ_0), the electric potential at channel midline (Φ_m) as well as the partition coefficient for monovalent co-ions. We report here the partition coefficient K for both a monovalent and divalent negatively charged tracer. The reason is that experimentally, we have used fluorescein dianion, which carries two charges near neutral pH, so that we report the K values not only for the fundamentally important monovalent co-ions, but also for our experimental tracer. The numerical simulation corresponds to the "solid nanochannel" model, including the estimation of the hydrogel swelling and ensuing pore size variation.

We find overall reasonable agreement for Φ_0 and Φ_m, the numerical simulation confirming indeed that Φ_0 is nearly independent of the gel concentration. We also find a reasonable agreement in terms of the partition coefficients K^{1-} and K^{2-}, with better performance for K values closer to 1. The notation "4.4e-2" is intended to mean $4.4*10^{-2}$.

Electric potential at alginate strands Φ_0 [mV]								
Gel	Numerical ("Solid nanochannel")				Analytical (Eq. S34)			
	1mM	10mM	100mM	1M	1mM	10mM	100mM	1M
25mg/mL	-217	-159	-101	-46	-238	-180	-123	-65
50mg/mL	-217	-159	-101	-46	-238	-180	-123	-65
65mg/mL	-217	-159	-101	-46	-238	-180	-123	-65

Electric potential at channel midlines Φ_m [mV]								
Gel	Numerical ("Solid nanochannel")				Analytical (Eq. S50 or S58)			
	1mM	10mM	100mM	1M	1mM	10mM	100mM	1M
25mg/mL	-1.33	-1.4e-3	-6e-8	-7e-20	-1.81	-1.9e-3	-8e-8	-1e-19
50mg/mL	-30	-1.4	-2.0e-3	-3e-10	-25	-1.9	-2.8e-3	-4e-10
65mg/mL	-49	-6.25	-4.4e-2	-4e-7	-65	-8.4	-6.1e-2	-6e-7

Partition coefficient for monovalent anion (co-ion): $\mathbf{K^{1-}}$								
Gel	Numerical ("Solid nanochannel")				Analytical (Eq. S63)			
	1mM	10mM	100mM	1M	1mM	10mM	100mM	1M
25mg/mL	0.59	0.82	0.91	0.96	0.58	0.83	0.91	0.97
50mg/mL	0.15	0.59	0.82	0.93	0.19	0.58	0.83	0.94
65mg/mL	0.073	0.44	0.76	0.91	0.039	0.40	0.77	0.92

Partition coefficient for monovalent anion (co-ion): $\mathbf{K^{2-}}$								
Gel	Numerical ("Solid nanochannel")				Analytical (Eq. S63)			
	1mM	10mM	100mM	1M	1mM	10mM	100mM	1M
25mg/mL	0.45	0.76	0.87	0.95	0.44	0.77	0.88	0.95
50mg/mL	0.035	0.45	0.76	0.91	0.054	0.44	0.77	0.91
65mg/mL	0.0080	0.27	0.67	0.87	0.0022	0.22	0.68	0.88

Table S64: Comparison between numerical evaluation of the Poisson-Boltzmann equation and analytical approximations.

Finally, in terms of numerical evaluation, eq. S63 used for the analytical calculation of the partition coefficients in Table S64 presents the difficulty that at the lower bound of $y=\Phi_m/V_{th}$, the term $(\cosh(y)-\cosh(\Phi_m/V_{th}))^{-1/2}$ diverges. To mitigate this problem, we use two complementary strategies. Firstly, it is necessary to adapt the step size dy values. Basically, the dy values need to be made sufficiently small such that the product $(\cosh(\Phi_m/V_{th}+dy)-\cosh(\Phi_m/V_{th}))^{-1/2}dy$ tends to zero for the y values closest to Φ_m/V_{th}. In practice, we use support points $y= \Phi_m/V_{th}+ (\Phi_0- \Phi_m)/V_{th}*\alpha$, where α is logarithmically spaced (i.e. of the type $\alpha=10^{-20},10^{-19}$, …$10^{-2},10^{-1}$, 1, with closer spacing in practice) such that the dy increase also exponentially as numerical summing proceeds. Second, given the very small difference between cosh(y) and $\cosh(\Phi_m/V_{th})$, for the y values closest to Φ_m/V_{th}, we used a linearized expression for the lower y values, since numerical imprecision will otherwise preclude successful evaluation of the small difference between cosh(y) and $\cosh(\Phi_m/V_{th})$.
For this, we proceeded with a Taylor development up to degree 2. We get:

$$\cosh(y)-\cosh(a)\approx \sinh(a)\cdot (y-a)+\cosh(a)\frac{(y-a)^2}{2} \qquad \text{(S65)}$$

Eq. S65 is then advantageously used in numerical evaluation of eq. S63 for points where |y-a|<<1, since it allows to directly plug the potentially very small (y-a) values, rather than calculating y separately for the evaluation of the cosh(y)-cosh(a) terms.

Software Implementation

We provide a software implementation of the algorithm outlined for the determination of the wall and midline potentials, as well as the partition coefficient described here. We do so in the "poisson.boltzmann.1D" package, available for download also as Electronic Supplementary Information (see Electronic Supplementary Information 5 for installation and usage instructions).

Specifically, different routines implement different aspects of the algorithm shown in Fig. S31, as shown in Table S66. We have kept the package as generic as possible, so rather than using the specific equations S50 and S58, we use their more generic versions S49 and S55 in the package. To obtain the partition coefficient from the hydrogel's physicochemical and the experimental parameters, one would use the high-level function "partition_coefficient_analytical_hydrogel" in the "poisson.boltzmann.1D" package.

Function in poisson.boltzmann.1D package	**Equation / Role**
potentials_analytical_nanochannel	Eq. S34, S40, S49, S55 (numerical solution), and Debye-Hückel approximation for very low potentials[2]
partition_coefficient_analytical_from_potentials	Eq. S63, Eq. S65
partition_coefficient_analytical_nanochannel	Coordinates the two functions above to enable single function call for getting the partition coefficient
partition_coefficient_analytical_hydrogel	Converts the hydrogel parameters to the nanochannel equivalent and calls "partition_coefficient_analytical_nanochannel" with the appropriate values

Table S66: Software implementation

Bibliography

1. J. T. Overbeek, *Prog Biophys Biophys Chem*, 1956, **6**, 57-84.
2. P. Debye and E. Hückel, *Physikalische Zeitschrift*, 1923, **24**, 185-206.
3. G. S. Manning, *Chem. Phys.*, 1969, **51**, 924.